JOC The Journal of Organic Chemistry

Article

pubs.acs.org/joc

Aromatic Ring Fused BOPHYs as Stable Red Fluorescent Dyes

Jun Wang, Qinghua Wu, Changjiang Yu, Yun Wei, Xiaolong Mu, Erhong Hao, and Lijuan Jiao*

The Key Laboratory of Functional Molecular Solids, Ministry of Education, Anhui Laboratory of Molecule-Based Materials, School of Chemistry and Materials Science, Anhui Normal University, Wuhu 241000, China

Supporting Information

ABSTRACT: Facile synthetic routes to a new class of red α-benzo-fused BOPHYs with 6,5,6,6,5,6-hexacyclic fused rings and β-thiophene-fused BOPHYs with 5,5,6,6,5,5-hexacyclic fused rings are presented. These dyes were characterized by NMR spectroscopy, HRMS, X-ray structure analysis, cyclic voltammetry, and optical measurements. Compared to parent BOPHY, significant red-shifts in the absorption (up to 600 nm in solution) and emission (up to 648 nm in solution and 717 nm in solid state), as well as high chemical stability and photostability, were found for these aromatic-ring-fused BOPHY dyes. As shown in cyclic voltammetry and DFT calculations, the aromatic ring fusions induced significantly increased HOMO energy levels, giving effective expansion of π-conjugation over these BOPHY dyes. These new molecular skeletons would be promising candidates for various applications in light of their unique structure and attractive photophysical properties.

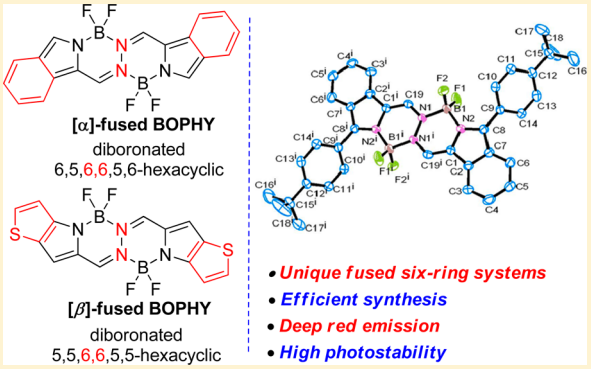

INTRODUCTION

Small organic fluorescent dyes have been the subject of ongoing investigation because of their diverse applications in medical and material sciences, including noninvasive bioimaging, molecular sensing, photothermal therapy, photovoltaic, optoelectronics, and laser optical recording.[1−3] Favorable properties, such as high chemical and photochemical stablilities, high molar absorption coefficients, high fluorescence quantum yields, large Stokes shifts, and tunable absorption/emission, are required for dyes to be suitable for these types of applications. Great efforts have been devoted to develop new dyes with a specific set of properties, including many organoboron-rigidified complexes.[4,5]

Recently, our and Ziegler's research groups[6] have independently developed the BF_2-complexed hydrazine−Schiff base linked bispyrroles, bis(difluoroboron)-1,2-bis((1*H*-pyrrol-2-yl)-methylene)hydrazine (BOPHY), in high yields from 2-formylpyrrole and hydrazine. The new fluorophore is rigidly planar and composed of four rings (5,6,6,5-tetracyclic rings), including two pyrrole rings at the periphery and two six-membered rings, each containing a BF_2 moiety (Figure 1).

Similar to the parent BODIPY (boron dipyrromethene) dyes[7,8] containing planar 5,6,5-tricyclic rings (Figure 1), BOPHY dyes also have a set of outstanding optical properties (including high molar absorption coefficients, high solution-state fluorescence quantum yields, highly tunable absorption/emission profiles, and excellent photostability) as well as good chemical versatility. Moreover, BOPHY dyes also have over 40 nm Stokes shifts and good solid-state fluorescence (ϕ up to 0.28),[6b] while BODIPYs generally suffer from small Stokes shifts of 7−15 nm and low solid-state fluorescence. The

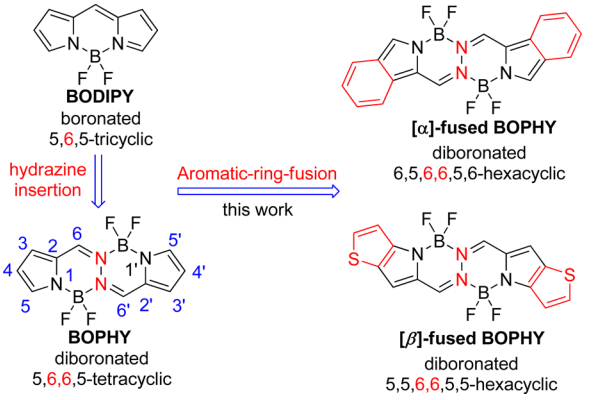

Figure 1. Chemical structures of BODIPY, BOPHY, and aromatic-ring-fused BOPHYs.

numbering system for the BOPHY skeleton with C_{2h} symmetry as defined by Ziessel and co-workers[9a] is slightly different from the BODIPY core. Interestingly, although BOPHY is more electron deficient than BODIPY,[8] its reported functionalizations such as halogenation,[9] formylation,[10] and Knoevenagel condensation[6b,9a,d,8,11a] are similar to those of BODIPYs. Because of their easy synthesis and excellent photophysical properties, BOPHY dyes have found wide applications as energy-transfer cascades,[9a,d,11a,b] photosensitizers for solar cells and photodynamic therapy,[9d,e] and fluorescence sensors[10,11c] in the last two years.

Received: September 17, 2016
Published: October 27, 2016

DOI: 10.1021/acs.joc.6b02291
J. Org. Chem. 2016, 81, 11316−11323

Scheme 1. Syntheses of α-Benzo-Fused BOPHYs 1a–c

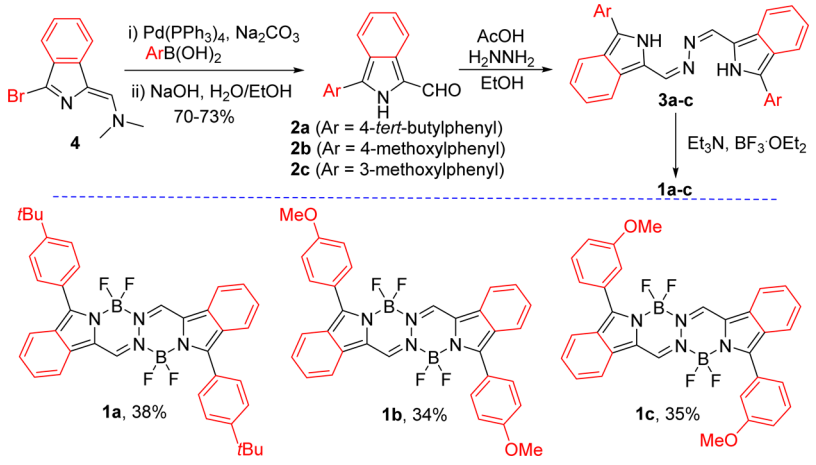

Scheme 2. Syntheses of β-Thiophene-Fused BOPHYs 1d and 1e

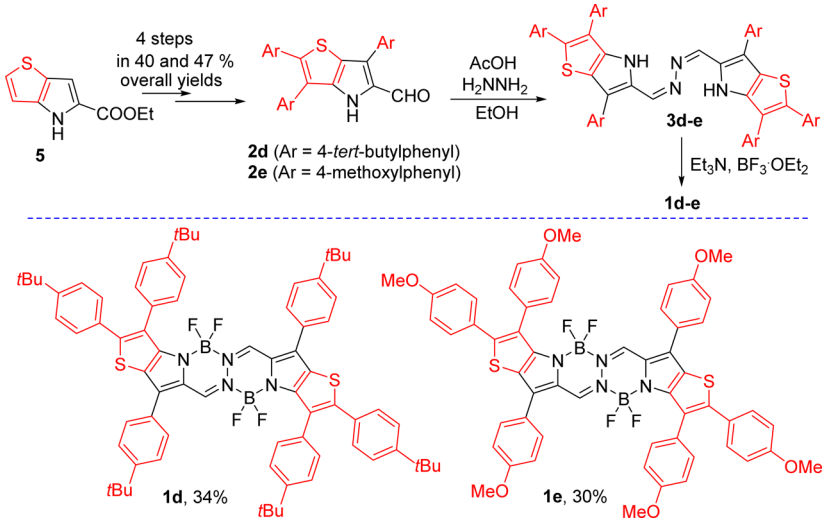

The emission wavelength of the simple BOPHY backbone[6b] (468 nm in dichloromethane) is shorter than that of the simple BODIPY backbone (526 nm in chloroform).[12] Linear extension at the 5,5′-positions of BOPHY by Knoevenagel condensation was an efficient way to red-shift its absorption and emission to the deep-red region.[6b,9a,d,8,11a] On the other hand, derivatives with extension of the π-conjugaton through aromatic ring fusion on the BOPHY core can be used as the basis of an alternative strategy for the introduction of a bathochromic shift, as succcessfully demonstrated in the corresponding BODIPY dyes.[13−18]

Herein, we report the efficient synthesis of a set of α-benzo-fused BOPHYs with 6,5,6,6,5,6-hexacyclic rings and β-thiophene-fused BOPHYs with 5,5,6,6,5,5-hexacyclic rings through the corresponding aromatic ring-fused precusors (Figure 1). These dyes show significant red-shifts in absorption and emission as well as high chemical stability and photo-stability in solution. While this manuscript was in preparation, Liu and Han's group reported the synthesis of three symmetrical β-furan-fused BOPHYs.[19]

RESULTS AND DISCUSSION

Syntheses. The synthetic route for α-benzo-fused BOPHYs **1a–c** is shown in Scheme 1. The key synthetic precursor 1-formylisoindoles **2a–c** were generated in 70–73% yields between compound **4** and various aryl boronic acids via the Suzuki coupling reaction (Scheme 1).[15] Subsequent acetic acid promoted condensation of **2a–c** with hydrazine in ethanol at room temperature gave hydrazine–Schiff base linked bisisoindoles **3a–c**, which were used directly for the subsequent BF_2 complexation without characterization after precipitation from the reaction mixture. The above one-pot (two-step) reactions successfully gave BOPHYs **1a–c** in 34–38% isolated overall yields (Scheme 1).

Recently, we reported a new class of NIR β-thiophene-fused boron difluoride azadipyrromethenes (AzaBODIPY) with sharp absorption and fluorescence emission bands at around 800 nm[18] that are longer than those of α-benzo-fused azaBODIPYs.[20] Thus, we wondered if extending the conjugation of the BOPHY system through fusion of the thiophene ring at β-position would be a suitable method for further extending the absorption/emission wavelength of BOPHY dyes.

The key synthetic precursors, α-formylthiophene-fused pyrroles **2d** and **2e**, were generated in four steps with 40 and 47% overall yields, respectively, from thienopyrrole **5** via bromination, the Suzuki coupling reaction, decarboxylation, and formylation reaction according to our previously reported methods (Scheme 2).[18]

DOI: 10.1021/acs.joc.6b02291
J. Org. Chem. 2016, 81, 11316–11323

Similar to the synthesis of **1a−c**, condensation of **2d** and **2e** with hydrazine and subsequent BF_2 complexation successfully gave β-thiophene-fused BOPHYs **1d** and **1e** in 34% and 30% yields, respectively, after column chromatography on silica gel (Scheme 2). BOPHYs **1a−e** were characterized by NMR and HRMS analysis. The structure of BOPHY **1a** was further confirmed by X-ray analysis (Figure 2).

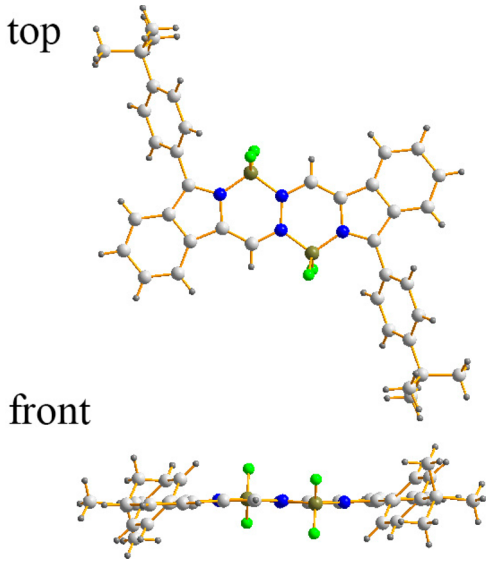

Figure 2. Top and front views of the X-ray structures of **1a**. Key: C, light gray; H, gray; N, blue; B, dark yellow; F, bright green.

X-ray Structure. Crystals of BOPHY **1a** suitable for X-ray analysis were obtained by slow evaporation of chloroform solution at room temperature and were characterized by X-ray crystallography as shown in Figure 2. There are six rigid planar ring structures in the chromophore of **1a**: two isoindole units at the periphery and two BF_2-containing six-membered rings in the center, with only the fluorine atoms and the phenyl substituents deviating from these chromophore planes. The average root-mean-square deviation of six planar rings in the BOPHY core is 0.0041 Å, indicating that **1a** adopts an almost planar conformation. The phenyl ring at the 5-position is tilted by 47.5° relative to the BOPHY core (Table S1, Supporting Information). The B−N bond lengths are 1.579(63) Å (hydrazino-nitrogen atom) and 1.536(69) Å (pyrrole-nitrogen atom) for compound **1a**, where these values are 1.599(23) and 1.515(31) Å, respectively, in the previously reported parent BOPHY **M**.[6b] The decreased distance of the two types of B−N bond lengths may indicate better conjugation in this benzo-fused BOPHY compared to the parent BOPHY **M**.

In the crystal-packing structure (Figure 3), **1a** showed a well-ordered (a slipped head-to-tail) two-dimensional structure due to $\pi-\pi$ and dipole−dipole interactions. The planes of the two molecules are almost parallel to each other, with a 3.52 Å mean distance between the two neighboring cores.

Spectroscopic Properties. The absorption and fluorescence emission spectra of dyes **1a−e** cover a broad range of the visible spectrum (Figure 4 and Figures S3−S7 in the Supporting Information), and their optical properties are summarized in Table 1.

Because of the extended π-conjugation, these BOPHYs have broad absorption bands with maxima of the main band ranging from 552 to 610 nm in different solvents, which are more than

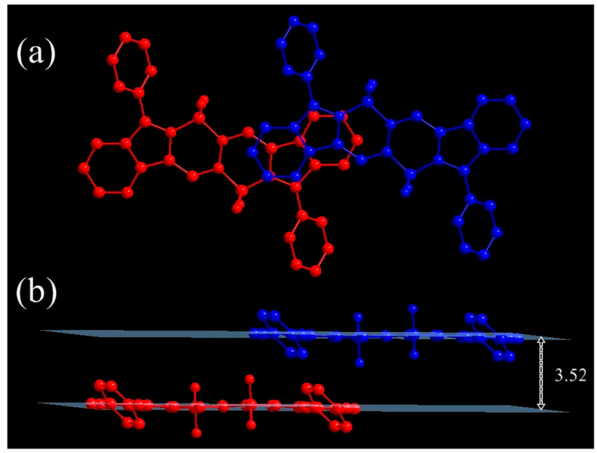

Figure 3. Top view (a) and side view (b) of intermolecular crystal packing of **1a**.

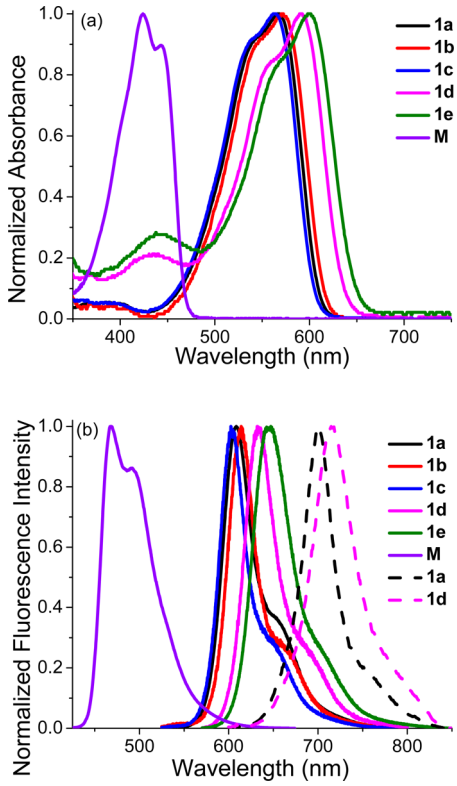

Figure 4. Normalized absorption (a) and fluorescence emission (b) spectra of BOPHYs **1a−e** and parent BOPHY **M** in dichloromethane (solid lines) and in solid state (dash lines).

the 140 nm bathochromic shift as compared to those of the corresponding parent BOPHY **M**. As shown in Figure 4a, BOPHYs **1a**, **1b**, and **1c** each have maximum absorption peaks at 567, 571, 563 nm in dichloromethane, respectively. β-Thiophene-fused BOPHYs **1d** and **1e** exhibit maximum absorption peaks at 591 and 600 nm in dichloromethane, respectively, which are over 20 nm red shift of the absorption maximum compared to those of α-benzo-fused BOPHYs **1a−c**, indicating a highly extended π-delocalization caused by fusion of the thieno ring at the BOPHY core.

Similar to the absorption, these dyes also showed red-shifted fluorescence in dichloromethane with maxima of the main band ranging from 602 to 648 nm, as shown in Table 1 and Figure

DOI: 10.1021/acs.joc.6b02291
J. Org. Chem. 2016, 81, 11316−11323

Table 1. Photophysical Properties of BOPHYs 1a−e at Room Temperature in Different Solvents

BOPHYs	solvent	λ_{abs}^{max}(nm)	λ_{em}^{max}(nm)	logε_{max}	Φ^a	Stokes Shift (cm^{-1})
M[14]	dichloromethane	423	468	4.60	>0.99	2300
1a	acetonitrile	557	601	4.78	0.26	1300
	DMF	566	607	4.79	0.28	1200
	dichloromethane	567	608	4.79	0.34	1200
	hexane	568	603	4.82	0.34	1000
	toluene	573	611	4.78	0.34	1100
1b	acetonitrile	561	606	4.73	0.22	1300
	DMF	569	613	4.69	0.23	1300
	dichloromethane	571	614	4.65	0.31	1200
	hexane	573	607	4.71	0.32	1000
	toluene	579	616	4.72	0.31	1000
1c	acetonitrile	552	596	4.77	0.24	1300
	DMF	561	603	4.74	0.27	1200
	dichloromethane	563	602	4.75	0.36	1200
	hexane	564	598	4.76	0.34	1000
	toluene	571	608	4.75	0.34	1100
1d	acetonitrile	574	627	4.85	0.49	1500
	DMF	584	636	4.66	0.45	1400
	dichloromethane	591	631	4.90	0.60	1100
	hexane	591	626	4.96	0.64	900
	toluene	596	632	4.90	0.59	1000
1e	acetonitrile	587	641	4.82	0.36	1400
	DMF	593	654	4.79	0.32	1600
	dichloromethane	600	648	4.88	0.50	1200
	hexane	595	630	4.85	0.46	900
	toluene	610	649	4.87	0.51	1000

[a]The fluorescence quantum yields were calculated using rhodamine B (ϕ = 0.49 in ethanol) as the standards for **1a−c** and cresyl violet perchlorate (ϕ = 0.54 in methanol) for **1d,e**, respectively. The standard errors are less than 10%.

4b. The fluorescence quantum yields of the dyes in various solvents were in the range of 0.22−0.64. In dichloromethane, the β-thiophene-fused BOPHYs **1d** and **1e** showed strong emissions in the deep red region (λ_{em} = 631 nm, Φ = 0.60) and (λ_{em} = 648 nm, Φ = 0.50), respectively (Table 1), while BODIPY **1a** with α-fusion of phenyl rings showed weaker emissions in the red region (λ_{em} = 608 nm, Φ = 0.34). Compared to parent BOPHY **M**,[6] the emission maximum of β-thiophene-fused BOPHY **1e** in dichloromethane showed an 180 nm bathochromic shift and a decreased fluorescent quantum yield at 0.50.

We further investigated the solvent-dependent photophysical properties of these BOPHYs. The increase of the solvent polarity from toluene to acetonitrile (Table 1 and Figures S3−S7 in the Supporting Information) leads to a slight blue-shift of the absorption and emission bands of BOPHYs **1a−e**. For example, the absorption maximum of BOPHY **1a** in toluene emerged at 573 nm and blue-shifted to 557 nm in acetonitrile, while the emission maximum of BOPHY **1a** in toluene exhibited at 611 nm and also blue-shifted to 601 nm in acetonitrile. Importantly, the fluorescence quantum yields of BOPHYs **1a−e** only showed a slight decrease from toluene to acetonitrile (Table 1).

Previously, we showed that BOPHY dyes are highly fluorescent in the solid state,[6b,21] in contrast to their BODIPY analogues. With these aromatic-ring-fused BOPHY dyes, solid-state fluorescence at the near-infrared regions, which is rare for organoboron materials,[22] is expected. Representative α-benzo-fused BOPHY **1a** and the β-thiophene-fused BOPHY **1d** were selected, and they both showed strong near-infrared fluorescence centered at 701 nm (ϕ = 0.10) and 717 nm (ϕ = 0.13) in the solid powder state, respectively (Figure 4b).

The photostabilities of BOPHYs **1a−e** in toluene were measured by continuous irradiation with a 500 W Xe lamp. Compared to a well-known commercial dye, 1,3,5,7-tetramethylBODIPY (4,4-difluoro-1,3,5,7-tetramethyl-4-bora-3a,4a-diaza-*s*-indocene), these BOPHYs show excellent photostability. During the period of strong irradiation (60 min), more than 97% of the amount of **1a−e** remained, while only 76% of 1,3,5,7- tetramethylBODIPY remained under the same conditions (Figure 5). This results are in agreement with our previously reported results for parent BOPHY **M**,[6b] indicating the high photostabilities of BOPHY dyes.

Electrochemical Properties. Cyclic voltammetry of **1a** and **1c** was performed in deoxygenated dichloromethane at room temperature containing tetrabutylammonium hexafluorophosphate ($TBAPF_6$) as the supporting electrolyte (Figure 6). BOPHYs **1a** and **1c** each display an irreversible reduction wave with E_{pc} at −1.19 and −1.14 V. One reversible oxidation wave was observed with half-wave potentials at 1.08 and 1.14 V (vs SCE) for **1a** and **1c**, respectively. HOMO energy levels of −5.38 and −5.48 eV and LUMO energy levels of −3.31 and −3.37 eV were estimated for **1a** and **1c**, respectively, based on their onset potential of the first oxidation and reduction waves. Notably, the fusion of benzo rings at the BOPHY core causes a large increase in the HOMO energy. Electrochemical energy band gaps for BOPHY **1a** and **1c** were calculated to be 2.07 and 2.11 eV, respectively, which is in good agreement with their optical band gaps. In comparison with the nonfused BOPHY **M**, the results indicate that the benzene-fused structure mainly

DOI: 10.1021/acs.joc.6b02291
J. Org. Chem. 2016, 81, 11316−11323

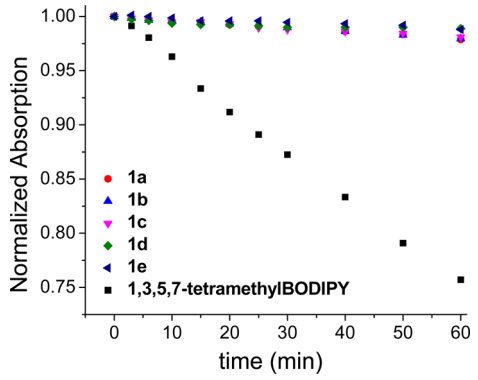

Figure 5. Comparison of the photostability of dyes BOPHYs **1a**–**e** and 1,3,5,7-tetramethylBODIPY in air-saturated toluene under continuous irradiation with a 500 W Xe lamp over 60 min; 35 mW·cm^{-2}; 25 °C.

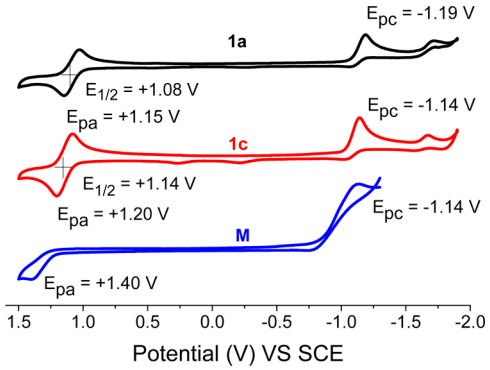

Figure 6. Cyclic voltammograms of 1 mM **1a**, **1c**, and **M** measured in dichloromethane solution containing 0.1 M $TBAPF_6$ as the supporting electrolyte at room temperature. Glassy carbon electrode as a working electrode, and the scan rate at 50 mV s^{-1}.

increases the HOMO energy levels and thus decreases the energy band gaps.[14d]

DFT Calculations. To further understand their electronic properties, the density functional theory (DFT) and time-dependent DFT (TDDFT) calculations were performed using a TPSSh/6-311G* basis set on BOPHY **M** and core-expanded BOPHYs **1a** and **1d** (the phenyl-substituted groups are replaced by hydrogen atoms). DFT calculations shows that BOPHYs **1a** and **1d** have similar electronic properties with parent **M**,[6a] C_{2h} geometries do not represent energy minima, and C_2 and C_i structures are the stationary points on the potential energy surfaces (Figure 7 and Figure S11 in the Supporting Information). Both HOMO and LUMO of BOPHYs **1a** and **1d** are well distributed over 6,5,6,6,5,6-hexacyclic fused rings and 5,5,6,6,5,5-hexacyclic fused rings, respectively (Figures 7 and Figure S11 in the Supporting Information). DFT calculations indicate that both the benzene fusion at the *a* bond and thiophene-fusion at the *b* bond in the BOPHY skeleton significatly increase their HOMO energy levels (Figures 7 and Figure S11 in the Supporting Information), while thiophene fusion at the *b* bond also slightly increases the LUMO energy level.[14d]

The TDDFT calculations on both BOPHYs **1a** and **1d** show strong absorption with the lowest energy mostly consisting of the HOMO–LUMO transition (Tables S3 and S4 in the Supporting Information). The TDDFT calculations predict that BOPHYs **1a** and **1d** are ~90 nm red-shift for the first excited state compared with parent BOPHY **M**, which is in good agreement with the experimental data.

CONCLUSION

In conclusion, we report an efficient synthesis of a series of *α*-benzo-fused BOPHYs with 6,5,6,6,5,6-hexacyclic rings and *β*-thiophene-fused BOPHYs with 5,5,6,6,5,5-hexacyclic rings through the corresponding aromatic-ring-fused precursors. These BOPHY fluorescent dyes are highly photostable and show excellent optical properties, including intensive absorption and emission within the range of 450–700 nm in solvent. In comparison with the parent BOPHY, these BOPHYs showed a more than 140 nm red-shift in both absorption and emission maximum. DFT calculations indicate the HOMO and LUMO orbitals are well distributed over 6,5,6,6,5,6-hexacyclic fused rings and 5,5,6,6,5,5-hexacyclic fused rings of these BOPHYs, respectively. As shown in cyclic voltammetry and DFT calculations, the aromatic ring fusions induced increased HOMO energy levels, giving effective expansion of *π*-

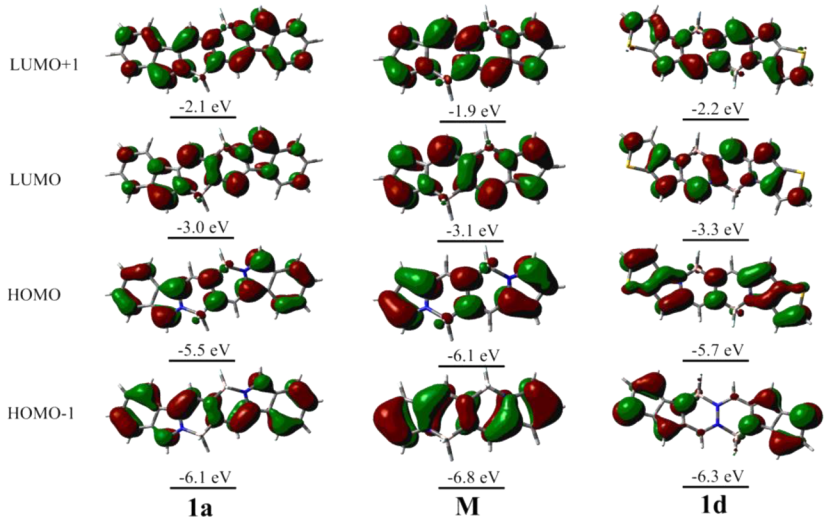

Figure 7. PCM-DFT calculated (TPSSh/6-311G(d)) frontier molecular orbital profiles of BOPHYs **1a**, **1d**, and **M** with C_2 symmetry. Phenyl substituents were omitted for clarity.

DOI: 10.1021/acs.joc.6b02291
J. Org. Chem. 2016, 81, 11316–11323

conjugation over these BOPHY dyes. The facile synthesis, the unique molecular skeletons, and their attractive photophysical properties point to possible applications of these new dyes in biotechnology and materials.

EXPERIMENTAL SECTION

General Methods. Reagents and solvents were used as received from commercial suppliers unless noted otherwise. All reactions were performed in oven-dried or flame-dried glassware unless otherwise stated and were monitored by TLC using 0.25 mm silica gel plates with UV indicator (HSGF 254) for thin-layer chromatography (TLC). Flash column chromatography was performed using silica gel (200−400 mesh). ^{1}H and ^{13}C NMR were recorded on a 300 or 500 MHz NMR spectrometer at room temperature. Chemical shifts (δ) are given in ppm relative to $CDCl_3$ (7.26 ppm for ^{1}H, 77 ppm for ^{13}C) or to internal TMS. High-resolution mass spectra (HRMS) were obtained using APCI-TOF in positive-ion mode.

Photophysical Measurements. UV−vis absorption and fluorescence emission spectra were recorded on commercial spectrophotometers (190−900 nm scan range) at room temperature (10 mm quartz cuvette). Relative fluorescence quantum efficiencies of BODIPY derivatives were obtained by comparing the areas under the corrected emission spectrum of the test sample in various organic solvents with with rhodamine B (Φ = 0.49 in ethanol)[23a] and cresyl violet perchlorate (Φ = 0.54 in methanol).[23b] Nondegassed, spectroscopic-grade solvents and a 10 mm quartz cuvette were used. Dilute solutions ($0.01 < A < 0.05$) were used to minimize the reabsorption effects. Quantum yields were determined using eq 1[24]

$$\Phi_x = \Phi_r \cdot \frac{F_x}{F_r} \cdot \frac{1 - 10^{-A_r(\lambda_{ex})}}{1 - 10^{-A_x(\lambda_{ex})}} \cdot \frac{n_x^2}{n_r^2} \quad (1)$$

where the subscripts x and r refer, respectively, to our sample x and reference (standard) fluorophore r with known quantum yield A_r in a specific solvent, F stands for the spectrally corrected, integrated fluorescence spectra, $A(\lambda_{ex})$ denotes the absorbance at the used excitation wavelength λ_{ex}, and n represents the refractive index of the solvent (in principle at the average emission wavelength). Absolute fluorescence quantum yields of **1a** and **1d** in powder solids (excited at 467 nm) of these dyes are measured using an integrating sphere[25] according to the definition of fluorescence efficiency.

Photostabilities. Photostabilities of BOPHYs **1a−e** (1×10^{-5} M) and 1,3,5,7-tetramethylBODIPY (1×10^{-5} M) in air-saturated toluene were studied under continuous irradiation with a 500 W Xe lamp over 60 min at 25 °C. Light intensity of 35 mW·cm^{-2} was used.

Cyclic Voltammograms. Cyclic voltammograms of 1 mM **2a** and **2c** were measured in dichloromethane solution containing 0.1 M $TBAPF_6$ as the supporting electrolyte, glassy carbon electrode as a working electrode, Pt wire as a counter electrode, and a saturated calomel electrode (SCE) as reference electrode at 50 mV s^{-1} as the scanning rate at room temperature.

Crystallography. Crystals of **1a** suitable for X-ray analysis were obtained by slow evaporation of chloroform solution at room temperature. A suitable crystal was chosen and mounted on a glass fiber using grease. Crystal diffraction suitable for X-ray analysis was performed on a CCD diffractometer using graphite-monochromated Mo Kα radiation (λ = 0.71073 Å) at 293(2) K with φ and ω scan techniques. An empirical absorption correction was applied using the SADABS program.[26] All structures were solved by direct methods, completed by subsequent difference Fourier syntheses, and refined anisotropically for all non-hydrogen atoms by full-matrix least-squares calculations based on F^2 using the SHELXTL program package.[27] The hydrogen atom coordinates were calculated with SHELXTL by using an appropriate riding model with varied thermal parameters. The residual electron densities were of no chemical significance. CCDC-1500818 (**1a**) contains the supplementary crystallographic data for this paper. These data can be obtained free of charge from the Cambridge Crystallographic Data Centre via www.ccdc.cam.ac.uk/data_request/cif.

Computational Details. The ground-state geometry was optimized by using the DFT method at the TPSSh/6-311G (d) level. The same method was used for vibrational analysis to verify that the optimized structures correspond to local minima on the energy surface. TD-DFT computations were used to obtain the vertical excitation energies and oscillator strengths at the optimized ground-state equilibrium geometries at the same level. The geometry optimizations of all of the molecules in dichloromethane were performed using the self-consistent reaction field (SCRF) method and the polarizable continuum model (PCM). All of the calculations were carried out by the methods implemented in the Gaussian 09 package.[28]

Synthesis. Compounds **2a−c**[15] and compounds **2d−e**[18] were synthesized according to the literature.

*General Procedure for the Preparation of BOPHYs **1a−c**.* To 10 mL of ethanol in a 100 mL round-bottom flask were added 1-formyl-3-arylisoindole **2** (1 mmol), 80% hydrazine (30 μL, 0.5 mmol), and acetic acid (100 μL). The reaction mixture was allowed to stir at room temperature, and TLC was used to follow the reaction. Upon completion of the reaction, 30 mL of cold water was added to the system to quench the reaction. The yellow precipitates were collected by filtration, washed with a small amount of water, and dried under vacuum to give brownish red solids. The resultant solid was dissolved in dry toluene (60 mL), and NEt_3 (1.5 mL) was added to the solution followed by dropwise addition of $BF_3{\cdot}OEt_2$ (2 mL). Then the reaction mixture was stirred at 90 °C for 12 h, washed with water (30 mL × 3), dried over anhydrous Na_2SO_4, and evaporated under vacuum. The crude product was purified by chromatography (silica gel, hexane/CH_2Cl_2 = 1/2, v/v) to afford BOPHYs **1a−c**.

BOPHY **1a** was prepared from compound **2a** (278 mg, 1 mmol) as a red solid in 38% yield (122 mg). ^{1}H NMR (300 MHz, $CDCl_3$): δ 8.36 (s, 2H), 7.87- 7.79 (m, 8H), 7.62 (d, J = 6.0 Hz, 4H), 7.54 (t, J = 7.5 Hz, 2H), 7.35 (t, J = 7.5 Hz, 2H), 1.42 (s, 18H). ^{13}C NMR (75 MHz, $CDCl_3$): δ 153.8, 149.2, 135.3, 130.1, 130.0, 127.6, 127.5(6), 125.9, 125.8, 124.0, 123.9(9), 118.4, 118.2, 35.4, 31.7, 31.6. HRMS (APCI): calcd for $C_{38}H_{36}B_2F_3N_4$ $[M - F]^+$ 627.3078, found 627.3072.

BOPHY **1b** was prepared from compound **2b** (252 mg, 1 mmol) as a red solid in 34% yield (101 mg). ^{1}H NMR (500 MHz, $CDCl_3$): δ 8.33 (s, 2H), 7.87 (d, J = 5.0 Hz, 4H), 7.84−7.81 (m, 4H), 7.54 (t, J = 5.0 Hz, 2H), 7.36 (t, J = 7.5 Hz, 2H), 7.13 (d, J = 5.0 Hz, 4H), 3.94 (s, 6H). ^{13}C NMR was not available due to poor solubility. HRMS (APCI): calcd for $C_{32}H_{24}B_2F_3N_4O_2$ $[M - F]^+$ 575.2037, found 575.2032.

BOPHY **1c** was prepared from compound **2c** (252 mg, 1 mmol) as a red solid in 35% yield (103 mg). ^{1}H NMR (500 MHz, $CDCl_3$): δ 8.37 (s, 2H), 7.86−7.83 (m, 4H), 7.55 (t, J = 7.5 Hz, 2H), 7.53−7.45 (m, 6H), 7.37 (t, J = 7.5 Hz, 2H), 7.13 (d, J = 5.0 Hz, 2H), 3.92 (s, 6H). ^{13}C NMR (125 MHz, $CDCl_3$): δ 160.0, 148.7, 135.2, 131.7, 131.5, 130.2, 130.0, 126.0, 123.9, 122.7, 118.3, 116.7, 115.4, 55.8. HRMS (APCI): calcd for $C_{32}H_{24}B_2F_3N_4O_2$ $[M - F]^+$ 575.2037, found 575.2032.

*General Procedure for the Preparation of BOPHYs **1d** and **1e**.* To ethanol (15 mL) and THF (5 mL) in a 100 mL round-bottom flask were added α-formylthiophene-fused pyrrole **2d** or **2e** (0.5 mmol), 80% hydrazine (15 μL, 0.25 mmol), and acetic acid (50 μL). The reaction mixture was left stir at room temperature, and TLC was used to follow the reaction. Upon completion of the reaction, 30 mL of cold water was added to the system to quench the reaction. The orange precipitates were collected by filtration, washed with a small amount of water, and dried under vacuum to give orange solids. The resultant solid was dissolved in dry toluene (60 mL), and NEt_3 (1 mL) was added to the solution, followed by dropwise addition of $BF_3{\cdot}OEt_2$ (1.2 mL). The reaction mixture was stirred at 90 °C for 12 h, washed with water (30 mL × 3), dried over anhydrous Na_2SO_4, and evaporated under vacuum. The crude product was purified by chromatography (silica gel, hexane/CH_2Cl_2 = 1/2, v/v) to afford **1d** and **1e**.

BOPHY **1d** was prepared from compound **2d** (247 mg, 0.5 mmol) as a coppery solid in 34% yield (101 mg). ^{1}H NMR (300 MHz, $CDCl_3$): δ 8.02 (s, 2H), 7.52 (brs, 8H), 7.42 (d, J = 9.0 Hz, 4H), 7.30 (d, J = 9.0 Hz, 4H), 7.31−7.13 (m, 8H), 1.37 (s, 18H), 1.36 (s, 18H),

DOI: 10.1021/acs.joc.6b02291
J. Org. Chem. 2016, 81, 11316−11323

1.26 (s, 18H). ^{13}C NMR (125 MHz, $CDCl_3$): δ 152.8, 152.2, 151.2 130.9, 130.7, 129.5, 129.4(6), 129.2, 129.0, 128.9, 126.9, 126.6, 126.0, 125.9(7), 125.7, 125.5, 35.2, 35.1, 35.0, 31.7, 31.6, 31.5. HRMS (APCI): calcd for $C_{74}H_{81}B_2F_3N_4S_2$ $[M - F + H]^+$ 1168.6041, found 1168.6061.

BOPHY **1e** was prepared from compound **2e** (252 mg, 0.5 mmol) as coppery solid in 30% yield (77 mg). ^{1}H NMR (300 MHz, $CDCl_3$): δ 8.00 (s, 2H), 7.51 (d, J = 9.0 Hz, 4H), 7.30 (brs, 4H), 7.16 (d, J = 9.0 Hz, 4H), 7.07 (d, J = 9.0 Hz, 4H), 6.75 (d, J = 9.0 Hz, 4H), 3.90 (s, 6H), 3.86 (s, 6H), 3.77(s, 6H). ^{13}C NMR was not available due to poor solubility. HRMS (APCI): calcd for $C_{56}H_{45}B_2F_3N_4O_6S_2$ $[M - F + H]^+$ 1012.2919, found 1012.2926.

■ ASSOCIATED CONTENT

Supporting Information

The Supporting Information is available free of charge on the ACS Publications website at DOI: 10.1021/acs.joc.6b02291.

Crystal structure data for **1a**, additional photophysical data and spectra, NMR spectra, high-resolution mass spectra, and additional computational data for all new compounds (PDF)

X-ray crystallographic data for **1a** (CIF)

■ AUTHOR INFORMATION

Corresponding Author

*E-mail: jiao421@ahnu.edu.cn.

Notes

The authors declare no competing financial interest.

■ ACKNOWLEDGMENTS

We thank the National Nature Science Foundation of China (Grant Nos. 21372011, 21402001, and 21672006) and the Nature Science Foundation of Anhui Province (Grant No. 1508085J07) for supporting this work. The numerical calculations in this paper have been performed on the supercomputing system in the Supercomputing Center of University of Science and Technology of China.

■ REFERENCES

(1) (a) Vendrell, M.; Zhai, D.; Er, J. C.; Chang, Y.-T. *Chem. Rev.* **2012**, *112*, 4391. (b) Kobayashi, H.; Ogawa, M.; Alford, R.; Choyke, P. L.; Urano, Y. *Chem. Rev.* **2010**, *110*, 2620. (c) Yuan, L.; Lin, W.; Zheng, K.; He, L.; Huang, W. *Chem. Soc. Rev.* **2013**, *42*, 622. (d) Fan, J.; Hu, M.; Zhan, P.; Peng, X. *Chem. Soc. Rev.* **2013**, *42*, 29. (e) Mei, J.; Leung, N. L. C.; Kwok, R. T. K.; Lam, J. W. Y.; Tang, B. Z. *Chem. Rev.* **2015**, *115*, 11718.

(2) (a) Yuan, L.; Lin, W.; Chen, H.; Zhu, S.; He, L. *Angew. Chem., Int. Ed.* **2013**, *52*, 10018. (b) Vázquez-Romero, A.; Kielland, N.; Arévalo, M. J.; Preciado, S.; Mellanby, R. J.; Feng, Y.; Lavilla, R.; Vendrell, M. *J. Am. Chem. Soc.* **2013**, *135*, 16018. (c) Choi, E. J.; Kim, E.; Lee, Y.; Jo, A.; Park, S. B. *Angew. Chem., Int. Ed.* **2014**, *53*, 1346. (d) Lei, Z.; Li, X.; Luo, X.; Zhou, M.; Yang, Y. *J. Org. Chem.* **2015**, *80*, 11538. (e) Shen, Y.; Shang, Z.; Yang, Y.; Zhu, S.; Qian, X.; Shi, P.; Zheng, J.; Yang, Y. *J. Org. Chem.* **2015**, *80*, 5906.

(3) (a) Bura, T.; Leclerc, N.; Fall, S.; Lévêque, P.; Heiser, T.; Retailleau, P.; Rihn, S.; Mirloup, A.; Ziessel, R. *J. Am. Chem. Soc.* **2012**, *134*, 17404. (b) Chen, J. J.; Conron, S. M.; Erwin, P.; Dimitriou, M.; McAlahney, K.; Thompson, M. E. *ACS Appl. Mater. Interfaces* **2015**, *7*, 662.

(4) Frath, G.; Massue, J.; Ulrich, G.; Ziessel, R. *Angew. Chem., Int. Ed.* **2014**, *53*, 2290.

(5) (a) Hapuarachchige, S.; Montaño, G.; Ramesh, C.; Rodriguez, D.; Henson, L. H.; Williams, C. C.; Kadavakkollu, S.; Johnson, D. L.; Shuster, C. B.; Arterburn, J. B. *J. Am. Chem. Soc.* **2011**, *133*, 6780. (b) Zhao, D.; Li, G.; Wu, D.; Qin, X.; Neuhaus, P.; Cheng, Y.; Yang, C.; Lu, Z.; Pu, X.; Long, C.; You, J. *Angew. Chem., Int. Ed.* **2013**, *52*, 13676. (c) Araneda, J.; Piers, W. E.; Heyne, B.; Parvez, M.; McDonald, R. *Angew. Chem., Int. Ed.* **2011**, *50*, 12214. (d) Kubota, Y.; Tanaka, S.; Funabiki, K.; Matsui, M. *Org. Lett.* **2012**, *14*, 4682. (e) Maeda, C.; Todaka, T.; Ema, T. *Org. Lett.* **2015**, *17*, 3090.

(6) (a) Tamgho, I.-S.; Hasheminasab, A.; Engle, J. T.; Nemykin, V. N.; Ziegler, C. J. *J. Am. Chem. Soc.* **2014**, *136*, 5623. (b) Yu, C.; Jiao, L.; Zhang, P.; Feng, Z.; Cheng, C.; Wei, Y.; Mu, X.; Hao, E. *Org. Lett.* **2014**, *16*, 3048. (c) Wang, L.; Tamgho, I.-S.; Crandall, L. A.; Rack, J. J.; Ziegler, C. J. *Phys. Chem. Chem. Phys.* **2015**, *17*, 2349.

(7) (a) Loudet, A.; Burgess, K. *Chem. Rev.* **2007**, *107*, 4891. (b) Ulrich, G.; Ziessel, R.; Harriman, A. *Angew. Chem., Int. Ed.* **2008**, *47*, 1184. (c) Boens, N.; Leen, V.; Dehaen, W. *Chem. Soc. Rev.* **2012**, *41*, 1130. (d) Zhao, J.; Xu, K.; Yang, W.; Wang, Z.; Zhong, F. *Chem. Soc. Rev.* **2015**, *44*, 8904.

(8) (a) Golf, H. R. A.; Reissig, H.; Wiehe, A. *J. Org. Chem.* **2015**, *80*, 5133. (b) Zhao, N.; Xuan, S.; Fronczek, F. R.; Smith, K. M.; Vicente, M. G. H. *J. Org. Chem.* **2015**, *80*, 8377. (c) Yu, C.; Wu, Q.; Wang, F.; Wei, Y.; Hao, E.; Jiao, L. *J. Org. Chem.* **2016**, *81*, 3761. (d) Ramírez-Ornelas, D.; Alvarado-Martínez, E.; Bañuelos, J.; Lopez Arbeloa, I.; Arbeloa, T.; Mora-Montes, H. M.; Pérez-García, L. A.; Peña-Cabrera, E. *J. Org. Chem.* **2016**, *81*, 2888. (e) Feng, Z.; Jiao, L.; Feng, Y.; Yu, C.; Chen, N.; Wei, Y.; Mu, X.; Hao, E. *J. Org. Chem.* **2016**, *81*, 6281. (f) Zhou, X.; Yu, C.; Feng, Z.; Yu, Y.; Wang, J.; Hao, E.; Wei, Y.; Mu, X.; Jiao, L. *Org. Lett.* **2015**, *17*, 4632.

(9) (a) Huaulmé, Q.; Mirloup, A.; Retailleau, P.; Ziessel, R. *Org. Lett.* **2015**, *17*, 2246. (b) Li, X.; Ji, G.; Son, Y. *Dyes Pigm.* **2016**, *124*, 232. (c) Dai, C.; Yang, D.; Zhang, W.; Bao, B.; Cheng, Y.; Wang, L. *Polym. Chem.* **2015**, *6*, 3962. (d) Zhang, C.; Zhao, J. *J. Mater. Chem. C* **2016**, *4*, 1623. (e) Cui, T.-F.; Zhang, J.; Jiang, X.-D; Su, Y.-J.; Sun, C.-L.; Zhao, J.-L. *Chin. Chem. Lett.* **2016**, *27*, 190.

(10) Li, Y.; Zhou, H.; Yin, S.; Jiang, H.; Niu, N.; Huang, H.; Shahzad, S. A.; Yu, C. *Sens. Actuators, B* **2016**, *235*, 33.

(11) (a) Rhoda, H. M.; Chanawanno, K.; King, A. J.; Zatsikha, Y. V.; Ziegler, C. J.; Nemykin, V. N. *Chem. - Eur. J.* **2015**, *21*, 18043. (b) Mirloup, A.; Huaulmé, Q.; Leclerc, N.; Lévêque, P.; Heiser, T.; Retailleau, P.; Ziessel, R. *Chem. Commun.* **2015**, *51*, 14742. (c) Jiang, X.-D.; Su, Y.; Yue, S.; Li, C.; Yu, H.; Zhang, H.; Sun, C.-L.; Xiao, L.-J. *RSC Adv.* **2015**, *5*, 16735.

(12) Arroyo, I. J.; Hu, R.; Merino, G.; Tang, B. Z.; Peña-Cabrera, E. *J. Org. Chem.* **2009**, *74*, 5719.

(13) For reviews, see: (a) Lu, H.; Mack, J.; Yang, Y.; Shen, Z. *Chem. Soc. Rev.* **2014**, *43*, 4778. (b) Ni, Y.; Wu, J. *Org. Biomol. Chem.* **2014**, *12*, 3774. (c) Boens, N.; Verbelen, B.; Dehaen, W. *Eur. J. Org. Chem.* **2015**, *2015*, 6577.

(14) (a) Uppal, T.; Hu, X.; Fronczek, F. R.; Maschek, S.; Bobadova-Parvanova, P.; Vicente, M. G. H. *Chem. - Eur. J.* **2012**, *18*, 3893. (b) Diaz -Moscoso, A.; Emond, E.; Hughes, D. L.; Tizzard, G. J.; Coles, S. J.; Cammidge, A. N. *J. Org. Chem.* **2014**, *79*, 8932. (c) Yamazawa, S.; Nakashima, M.; Suda, Y.; Nishiyabu, R.; Kubo, Y. *J. Org. Chem.* **2016**, *81*, 1310. (d) Wakamiya, A.; Murakami, T.; Yamaguchi, S. *Chem. Sci.* **2013**, *4*, 1002.

(15) (a) Yu, C.; Xu, Y.; Jiao, L.; Zhou, J.; Wang, Z.; Hao, E. *Chem. - Eur. J.* **2012**, *18*, 6437. (b) Jiao, L.; Yu, C.; Liu, M.; Wu, Y.; Cong, K.; Meng, T.; Wang, Y.; Hao, E. *J. Org. Chem.* **2010**, *75*, 6035. (c) Wang, J.; Wu, Q.; Xu, Y.; Yu, C.; Wei, Y.; Mu, X.; Hao, E.; Jiao, L. *RSC Adv.* **2016**, *6*, 52180.

(16) Umezawa, K.; Nakamura, Y.; Makino, H.; Citterio, D.; Suzuki, K. *J. Am. Chem. Soc.* **2008**, *130*, 1550.

(17) (a) Awuah, S. G.; Polreis, J.; Biradar, V.; You, Y. *Org. Lett.* **2011**, *13*, 3884. (b) Mahmood, Z.; Zhao, J. *J. Org. Chem.* **2016**, *81*, 587. (c) Sun, Z.; Guo, M.; Zhao, C. *J. Org. Chem.* **2016**, *81*, 229. (d) Zhou, X.; Wu, Q.; Feng, Y.; Yu, Y.; Yu, C.; Hao, E.; Wei, Y.; Mu, X.; Jiao, L. *Chem. - Asian J.* **2015**, *10*, 1979.

(18) (a) Wu, Y.; Cheng, C.; Jiao, L.; Yu, C.; Wang, S.; Wei, Y.; Mu, X.; Hao, E. *Org. Lett.* **2014**, *16*, 748. (b) Wang, J.; Li, J.; Chen, N.; Wu, Y.; Hao, E.; Wei, Y.; Mu, X.; Jiao, L. *New J. Chem.* **2016**, *40*, 5966.

(19) Zhou, L.; Xu, D.; Gao, H.; Zhang, C.; Ni, F.; Zhao, W.; Cheng, D.; Liu, X.; Han, A. *J. Org. Chem.* **2016**, *81*, 7439.

DOI: 10.1021/acs.joc.6b02291
J. Org. Chem. 2016, 81, 11316−11323

(20) (a) Donyagina, V. F.; Shimizu, S.; Kobayashi, N.; Lukyanets, E. A. *Tetrahedron Lett.* **2008**, *49*, 6152. (b) Lu, H.; Shimizu, S.; Mack, J.; Shen, Z.; Kobayashi, N. *Chem. - Asian J.* **2011**, *6*, 1026. (c) Gresser, R.; Hummert, M.; Hartmann, H.; Leo, K.; Riede, M. *Chem. - Eur. J.* **2011**, *17*, 2939.
(21) Gai, L.; Xu, J.; Wu, Y.; Lu, H.; Shen, Z. *New J. Chem.* **2016**, *40*, 5752.
(22) Cheng, X.; Li, D.; Zhang, Z.; Zhang, H.; Wang, Y. *Org. Lett.* **2014**, *16*, 880.
(23) (a) Benson, R. C.; Kues, H. A. *Phys. Med. Biol.* **1978**, *23*, 159. (b) Magde, D.; Brannon, J. H.; Cremers, T. L.; Olmsted, J. *J. Phys. Chem.* **1979**, *83*, 696.
(24) Lakowicz, J. R. *Principles of Fluorescence Spectroscopy*, 3rd ed.; Springer: New York, 2006.
(25) Massue, J.; Frath, D.; Retailleau, P.; Ulrich, G.; Ziessel, R. *Chem. - Eur. J.* **2013**, *19*, 5375.
(26) Sheldrick, G. M. *SADABS: Program for Empirical Absorption Correction of Area Detector Data*; University of Göttingen: Germany, 1996.
(27) Sheldrick, G. M. *SHELXTL 5.10 for Windows NT: Structure Determination Software Programs*; Bruker Analytical X-ray Systems, Inc.: Madison, WI, 1997.
(28) Frisch, M. J.; Trucks, G. W.; Schlegel, H. B., et al. *Gaussian 09*, Revision B.01; Gaussian Inc.: Wallingford, CT, 2010.

DOI: 10.1021/acs.joc.6b02291
J. Org. Chem. 2016, 81, 11316−11323